

Incorporating a new wicking geotextile in northern, low volume highways to mitigate pavement edge cracking

Allan H. Bradley, R.P.F., P.Eng., Associate Research Leader, Roads and Infrastructure Group, FPIinnovations.

Papa-Masseck Thiam, Ing., M.Sc., Researcher, Roads and Infrastructure Group, FPIinnovations.

Stuart Drummond, Senior Project Coordinator, Transportation Engineering Branch, Highways and Public Works, Yukon Government.

Paul Murchison, P.Eng., Director, Transportation Engineering Branch, Highways and Public Works, Yukon Government.

René Laprade, P.Eng., Engineering Business Manager, Eastern Canada, TenCate Geosynthetics.

Paper prepared for presentation
at the *Innovation in Geotechnical and Materials Engineering* Session

of the 2017 Conference of the
Transportation Association of Canada
St. John's, NL

ABSTRACT

Longitudinal edge cracking is a widespread and costly safety concern for northern regulators, such as Yukon Highways and Public Works. The exact cause of longitudinal edge cracking in northern, low volume highways is not well understood. There are many factors that may be linked to cracking such as weak materials under the side slope toe, differential frost heave, oversteepened side slopes, concentration of moisture in road edge materials, and climate change. In an effort to prevent edge cracking in its low volume pavements, the Yukon Government partnered with FPIInnovations and TenCate in 2015 and 2016 to construct two, instrumented, thin pavement test sites on the Campbell Highway near Watson Lake, Yukon. The test pavements were reinforced with a new geosynthetic product; instrumentation installed above and below the geotextile monitored roadbed moisture content and temperature. Mirafi® H₂Ri is a high strength, woven, geotextile with hygroscopic, hydrophilic, and wicking properties that promote rapid drainage. It is anticipated that the geotextile will help prevent edge cracking by interrupting capillary rise from the subgrade, draining excess moisture from thawing layers, providing additional structural support, and confining road edge materials. Additional benefits may include the mitigation of rutting, cracking and pot holes associated with excess roadbed moisture. Activities in 2015 comprised site construction, and monitoring of moisture and temperature trends. The shoulders of the test pavement sections were consistently wetter than near centerline before and after paving. The geotextile, installed at the subbase-subgrade interface, reduced moisture in the subbase of both test pavements by up to 3%. In 2016, activities included continuing to evaluate roadbed moisture control by the geosynthetic, and assessing how well the new pavement design controls edge cracking and other pavement distresses. This innovative research will provide knowledge to owners, designers, and maintainers of low volume northern roads about road construction solutions to mitigate pavement distress, improve safety, and decrease maintenance costs.

Key words: Edge cracking, Mirafi® H₂Ri, geosynthetics, northern roads, low volume, instrumentation, design, drainage

INTRODUCTION

Some thin-surfaced low volume pavements in the north develop a unique form of edge cracking—the causes of which are not well understood. Figure 1 illustrates edge cracking in northern Canada.



Figure 1. Edge cracking can be wide, deep and extensive.

The extensive length, width and depth of this edge cracking create structural problems for the roads and can be costly to repair. In 2014, the Yukon Government, Department of Highways and Public Works (HPW) identified six locations on the Campbell Highway on which to try mitigating edge cracking with a new geosynthetic product from TenCate. This product, called Mirafi® H₂Ri, is able to rapidly drain wet roadbed soils and resist shearing, and this may prevent edge crack formation. In 2015, HPW partnered with FPIInnovations and TenCate to create two instrumented sites with which to study the effectiveness of Mirafi® H₂Ri to mitigate edge cracking and control roadbed moisture. This paper discusses potential causes of the failure mechanism, provides details about the construction of the two instrumented sites, and summarizes findings to-date at the test sites. This paper also discusses the ability of the fabric to drain water, increase road bearing capacity and to prevent edge cracking, and associated surface distresses, for northern low volume thin pavements.

SUMMARY OF LITERATURE ON THE POTENTIAL CAUSES OF EDGE CRACKING IN NORTHERN ROADS

According to HPW, edge cracking in northern roads is caused by lateral and vertical displacement of the road shoulders and side slopes. This displacement results from differential frost heave and thawing of the side slope and concentration of moisture in the road edge materials due to road surface drainage penetrating downwards along the edge of the bituminous surface and moisture wicking upwards with capillary action. Edge cracking has been observed in embankments, transition zones (cuts to fills, fills to cuts), through-cuts, realignments, and wet areas. Cracking may penetrate into the subbase materials; in some areas, cracking may penetrate into the subgrade by about 50 mm. Edge cracking occurs within 2 to 5 years of road construction.

Structural problems related to road construction in northern climates could be attributed to weak, uncompacted shoulder and side slope materials. Road shoulders and side slopes are difficult to compact and do not achieve the same density levels as materials under the running lanes. The under-compacted condition of these materials increases their hydraulic conductivity and causes them to intercept and retain more road surface runoff. It is noted that if the subgrade materials under the toe of the side slope are weak, or are weakened by high moisture levels, they will be inadequate to support the road edge and this also can lead to a rotation and spreading of the embankment. Edge cracking also can occur if road edge materials are too weak to support heavy vehicles driving along the road shoulder.

Frost heave occurs in soils that are subject to prolonged freezing temperatures (subzero temperatures), contain sufficient water and are frost susceptible. As previously described, road shoulder and side slope materials may have relatively high moisture contents because of differential compaction, capillary action and inadequate drainage. Silty and clayey subgrade soils are particularly problematic in their ability to conduct water from far below the road.

The maintenance practice of ploughing snow from the running surface casts snow into the ditches and right-of-way. When a roadside berm accumulates and starts to prevent the efficient casting of snow a grader with a side-mounted blade (a wing) is deployed to cut down the berm and push it further down the side slope towards the ditch line. Differential thawing may occur from this.

Bringing these concepts together, **edge cracking** occurs when loosely compacted road shoulders and side slopes rotate and spread outward. The resulting cracks can extend below the finished road shoulder by 0.75–0.80 m and marginally (50 mm) into the subgrade roadbed. Rotation and spreading may result from weak materials under the side slope toe, differential frost heave and thawing, oversteepened side slopes, and concentration of moisture in the road edge materials. Differential frost heave and thawing at the road edge are promoted by prolonged exposure to snow, and to a heightened moisture content in

the subgrade soils and subbase materials; and, soil displacement is exacerbated by a loosely compacted condition and over-steepened geometry of the side slope.

TEST SITE

Location

Over the last few years, portions of reconstructed highway between km 30.7- 42.2 of the Campbell Highway were observed to have moisture issues during the spring and early summer. Persistent problems were observed in six areas within the recent 2009-2010 construction project. These areas of interest were named sites 1-6. Two of those 6 sites (sites 4 and 6), located approximately 40 km north of Watson Lake, Yukon along the Campbell Highway (Figure 2), were chosen for this study. Both sites have muskeg vegetation and soils beside them. It is located in the transition between an area with discontinuous permafrost (50-90% of the area) and a low amount of ground ice (0-10% by volume in the upper 10-20 m of the ground) and a mountainous area to the north with sporadic permafrost (10-50% of the area) and a medium amount of ground ice (10-20% by volume).

Site Conditions

Site 4 has an elevation of 810 m. The site is located on a tangent near km 40.5, and has a profile grade of -2.8% (sloping downwards to the north). This site is in a wet depression and soils on the east side of the road were saturated during construction. Edge cracking extended for the entire 43-m length of the site on the east shoulder, and two parallel 15-m-long cracks were in the western shoulder.

Site 6 has an elevation of 822 m. Site 6 is located on a tangent near km 40.9, and has a profile grade of 2.7% (sloping downwards to the south). Edge cracking extended for the entire 43-m length of the site on the east shoulder, and one 9-m-long crack was in the western shoulder at the north end.

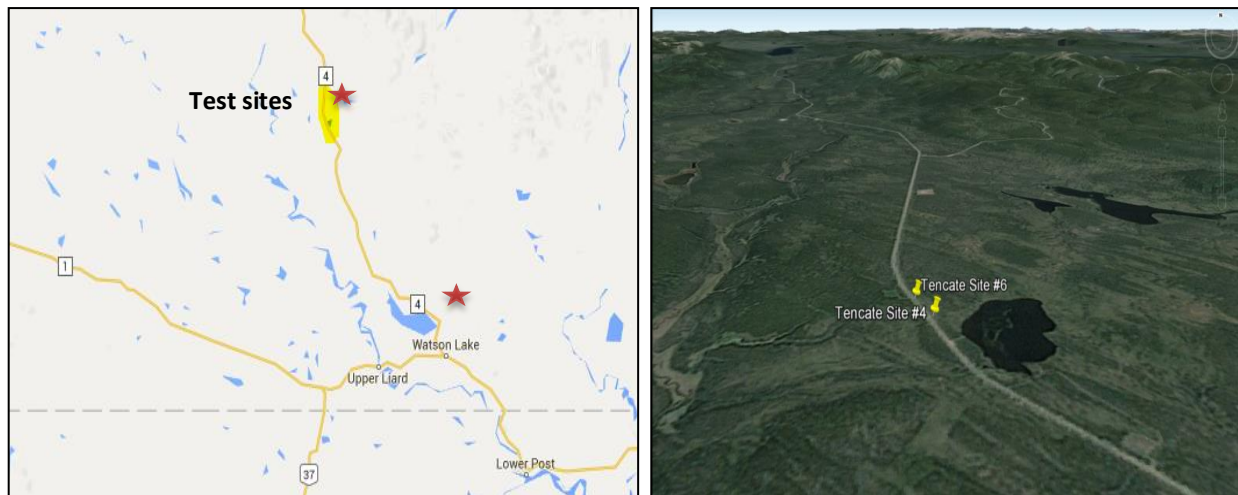


Figure 2. Test sites are located about 40 km north of Watson Lake on Highway 4 in southwest Yukon.

Road structure

Table 1 summarizes the road structure and dimensions at test sites 4 and 6.

Table 1. Road parameters

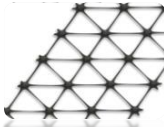
	Thickness (mm)	Description
Surface treatment	20-25	Granular A-type gravel in emulsified asphalt (HF, 250S)
Granular base	150	Granular A (20-mm crush)
Subbase	600	Granular E (200-mm pit run)
Subgrade	Ripped weathered rock	
Original Ground	(USCS classification SM) Silty gravelly sand (site 4); silty sand and gravelly silty sand (site 6)	
Road Prism	5.25 m lane width; 4% cross slope (treated as a low volume road); 3:1 side slopes for fills under 2 m high	

GEOSYNTHETICS AND INSTRUMENTATION

Geosynthetic

Per TenCate product literature, Mirafi® H₂Ri is capable of separation, filtration, soil reinforcement, confinement, and drainage. The geosynthetic has special hydrophilic and hygroscopic 4g yarn that provides wicking action through the plane of the geosynthetic. It offers soil and base course confinement resulting in greater load distribution, and robust damage resistance for stress installations. Table 2 summarizes the similarities and differences of Mirafi® H₂Ri with other geosynthetics.

Table 2. Comparison of important properties of various types of geosynthetics with Mirafi® H₂Ri

Function	Woven geotextile	High strength woven geotextile	Geogrid	Perforated Geocell	H2Ri Wicking Fabric
					
Filtration		✓✓			✓✓
Drainage		✓		✓✓	✓✓
Separation	✓✓	✓✓	✓		✓✓
Confinement	✓	✓	✓✓	✓✓✓	✓
Wicking					✓✓
Reinforcement	✓	✓✓✓	✓✓	✓✓✓	✓✓✓
Purchase price	\$	\$\$	\$	\$\$\$	\$\$

Thermistors

The thermistors were manufactured by Measurement Specialities, Inc. and the type was Epoxy Encapsulated Precision Interchangeable NTC thermistors that utilize high stability pressed-disk ceramic sensors for general applications. Four thermistors were arranged in a single sealed main string at specified separations. Five other thermistors were installed at the heads of individually sized cables (called fly outs) and the tails of these were all attached to the main string. A tenth thermistor was inserted in a radiation shield assembly and used to measure air temperature at the remote datalogger housing.

Moisture sensors

GS-1 moisture sensors, manufactured by Decagon Devices, Inc, were used for this study. The GS-1 moisture sensors are manufactured to tight tolerances and have been shown to have negligible between-sensor variation. Using a general soil calibration equation, the sensor readings are estimated to be ± 3 . A GS-1 moisture sensor was calibrated, per manufacturer's recommendations, using site 4 subgrade soils.

Data acquisition and software

Lakewood Systems Ltd.'s Ultralogger datalogger was used to collect data from the 16 site sensors (6 GS-1 moisture sensors, 10 epoxy 44007 NTC thermistors). A long life lithium battery was used as the system's power. The software used to program and communicate with sensors, and process and display data is called Prolog2 Datalogger Software version 2.226. This is a proprietary software developed and distributed by Lakewood Systems Ltd. Table 3 illustrates moisture sensor, thermistor and datalogger specifications.

Table 3. Moisture sensor, thermistor and specifications

	Range of measurement	Accuracy	Approximate cost (excl. taxes and shipping)
Decagon GS-1	0% to 57% VWC	1% to 2% (with soil-specific calibration)	\$120 (CDN)
Epoxy 44007 NTC Thermistor	-55° to 150° C	$\pm 0.2^\circ$ C	\$67 (cable, shipping, taxes, extra)
Datalogger	-50° to 50° C	-	\$3300

INSTALLATION

Geosynthetic Installation

The 3.4-m-wide strips of Mirafi[®] H₂Ri geosynthetic were rolled out on the subgrade starting at the road side slope. The outer edge of the geosynthetic was treated in one of three ways (see Figure 3 and Figure 4). A 22-m-long drain pipe made from slit, 2" ABS pipe was attached along the outside edge of the geosynthetic. The edge geosynthetic was draped vertically into the trench. The drain pipe was sloped at about 1% towards the outlet by skewing the geosynthetic strip. The drain pipe was drained with a pipe extension angled out of the trench outlet (SW quadrant of site 6, SE and SW quadrants of site 4). The long edge of the geosynthetic was draped down the 3:1 side slope and then covered with a minimum layer of shoulder material (NW, NE and SE quadrants of site 6). The geosynthetic was run horizontally to

the surface of the side slope and the edge barely covered with shoulder material (NE and NW quadrants of site 4). After the first strip of geosynthetic was installed along the road edge, a second strip was laid beside it, using at least 1 m of overlap. The topmost strip of geosynthetic was installed along centreline and overlapped the adjacent strips to either side (like a ridge cap shingle on a roof). This arrangement is intended to wick moisture from the centreline downslope towards the shoulders and provide reinforcement against cracking, separation of subgrade and subbase, and other product functions. Figure 5 shows an example of geosynthetics installation.

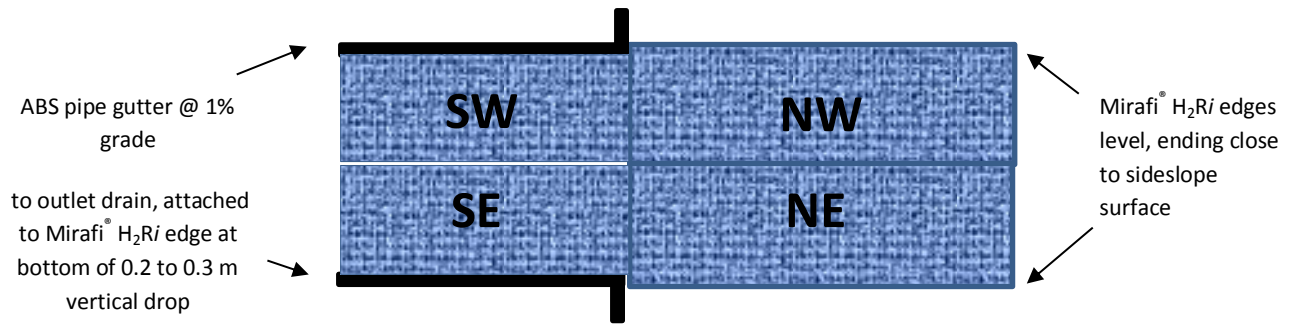


Figure 3. Edge treatments, by quadrant, for Mirafi[®] H₂Ri geosynthetic at test site 4.

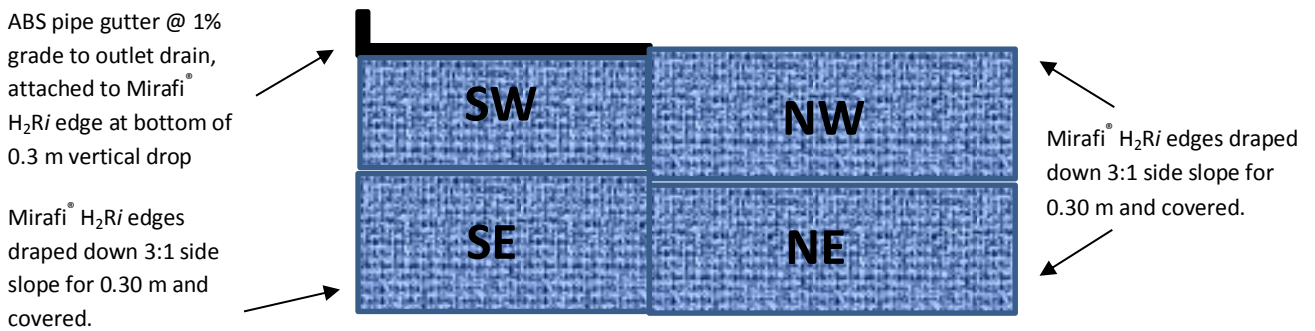


Figure 4. Edge treatments, by quadrant, for Mirafi[®] H₂Ri geosynthetic at test site 6.



Figure 5. Mirafi[®] H₂Ri edge in drain pipe hanging in trench at 1% slope

Instrumentation installation and road reconstruction

On site, the sensors were laid out according to site plans in the SE quadrant of site 4 and the NE quadrant of site 6. Then the remote datalogger housing tubes were installed in the right-of-way. A 0.3-m-deep trench was dug in the right-of-way and the cabling run from the remote datalogger housing to the road prism prior to backfilling this trench. The main thermistor string was routed across the subgrade surface and down one side of the augered hole near road centreline. The augered hole was then backfilled, carefully tamping native materials in-place around the thermistor string until the backfill material was level with the subgrade. Other thermistors and moisture sensors intended for below the geosynthetic were deployed on the subgrade surface at the road shoulder. Sensors intended for elevations above the geosynthetic were mounted on wooden stakes at the appropriate heights at centreline and road shoulder prior to installing the geosynthetic in the quadrant and around the stakes. Granular E materials were then dumped close to the staked sensors and manually shovelled into place in lifts around the sensors. Table 4 summarizes the instrumentation installed at sites 4 and 6. The geosynthetic at both sites was installed on top of the subgrade at a depth of 69 cm at site 4 and at a depth of 79 cm at site 6. The instrumentation arrangement was identical at site 6 except that the below-Mirafi® H2Ri moisture sensors were all located at a depth of 80 cm. After installing the geosynthetic and instrumentation (in quadrant SE in site 4 and quadrant NE in site 6), the road was reconstructed by placing and compacting in-place lifts of “Granular E” specification subbase material. Over this, 150 mm of “Granular A”-specification base material was placed, shaped to a 4% crown, watered and compacted in-place. In October (about 1 month later), the gravel surface was regraded in preparation for freeze-up. Following the instrumentation installation, test sites 4 and 6 were left unpaved until mid-June of 2016. On June 15, 2016, the test sites were surfaced with Bituminous Surface Treatment (BST).

Figure 6 and Figure 7 present the as-built arrangements of instrumentation at the two test sites.

Table 4. Summary of instrumentation at site 4 and 6

Site 4	Instrumentation at centreline	Instrumentation at road shoulder	Instrumentation at road shoulder - control section (no Mirafi® H ₂ Ri)
Thermistors	3 above Mirafi® H ₂ Ri (at 15, 30, 45 cm) 4 below Mirafi® H ₂ Ri (at 70, 100, 130, 160 cm)	1 below Mirafi® H ₂ Ri (at 70 cm)	1 thermistor at 70 cm
Moisture sensors	1 above Mirafi® H ₂ Ri (at 30 cm) 1 below Mirafi® H ₂ Ri (at 70 cm)	1 above Mirafi® H ₂ Ri (at 40 cm) 1 below Mirafi® H ₂ Ri (at 70 cm)	1 moisture sensor at 40 cm 1 moisture sensor at 70 cm
Site 6			
Thermistors	3 above Mirafi® H ₂ Ri (at 15, 30, 45 cm) 4 below Mirafi® H ₂ Ri (at 80, 110, 140, 170 cm)	1 below Mirafi® H ₂ Ri (at 80 cm)	1 thermistor at 80 cm
Moisture sensors	1 above Mirafi® H ₂ Ri (at 40 cm) 1 below Mirafi® H ₂ Ri (at 80 cm)	1 above Mirafi® H ₂ Ri (at 40 cm) 1 below Mirafi® H ₂ Ri (at 80 cm)	1 moisture sensor at 40 cm 1 moisture sensor at 80 cm

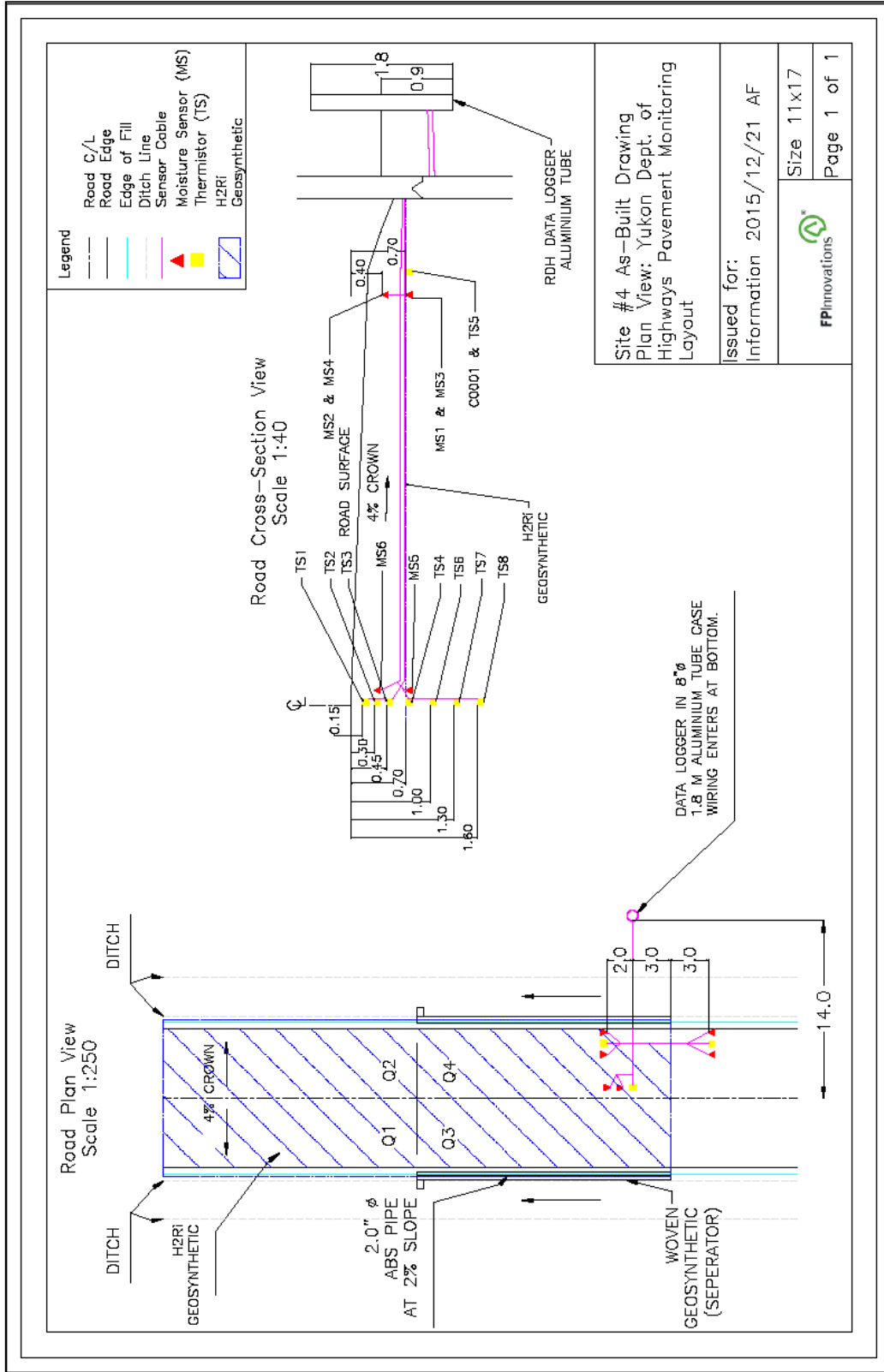
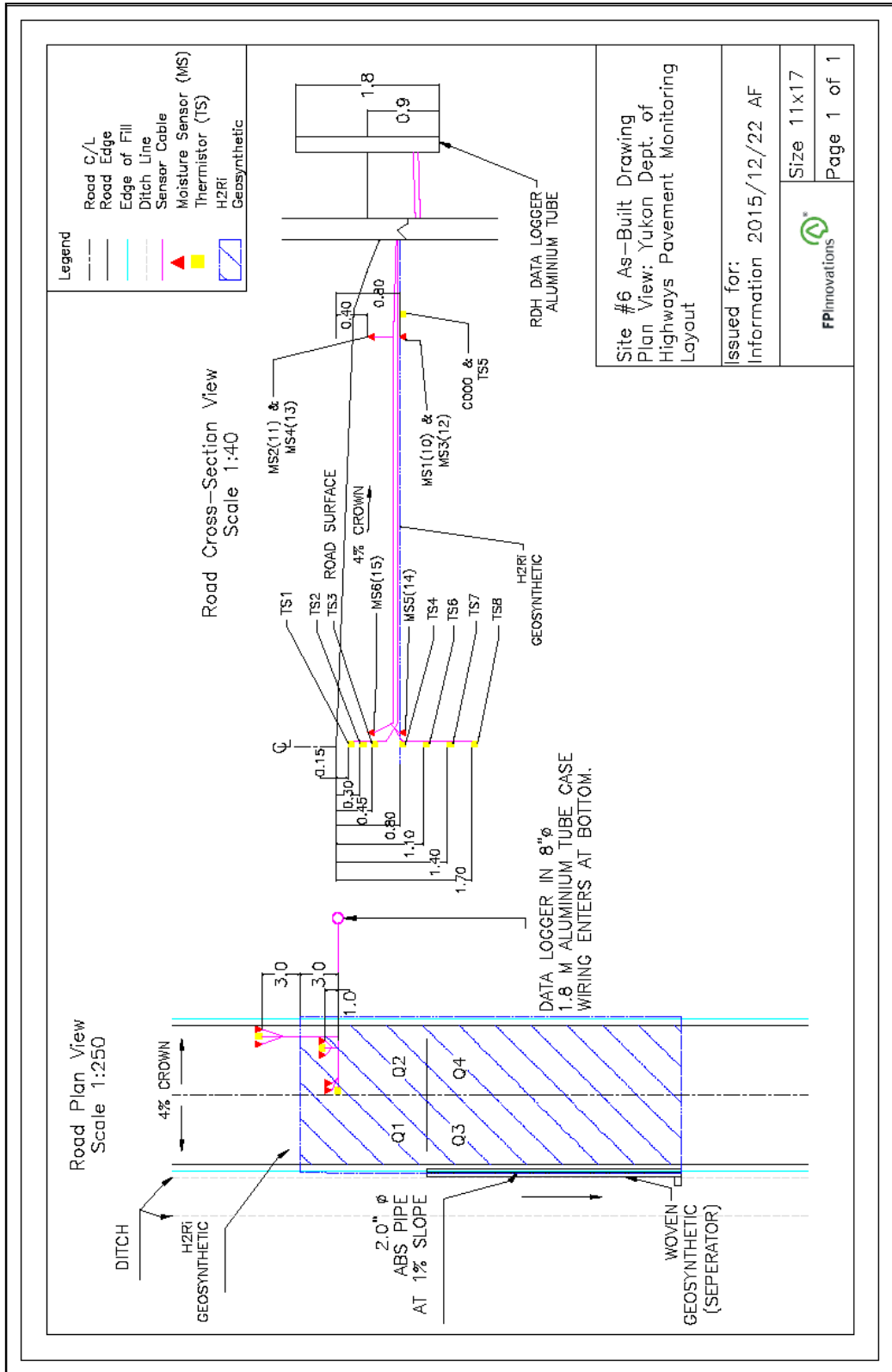


Figure 6. As-built drawing of site 4 instrumentation.



Site #6 As-Built Drawing
 Plan View; Yukon Dept. of
 Highways Pavement Monitoring
 Layout

Issued for:
 Information 2015/12/22 AF

Size 11x17
 Page 1 of 1

FPinnovations

Figure 7. As-built drawing of site 6 instrumentation.

RESULTS ANALYSIS

Following sites construction and instrumentation installation, the data loggers at two test sites (4 and 6) were manually downloaded, at approximately 2-month intervals between fall 2015 and winter 2017, to document changes in roadbed moisture and temperature. Both sites were frequently monitored for edge cracking and surface distress both before and after the application of BST. The moisture and temperature data from the test sites were analyzed for trends and relations. Moreover, a site visit was conducted in September 2016 to review 2015 activities, survey pavement distress at and near sites 4 and 6, review other parts along the highway subject to edge cracking, and discuss potential causes of edge cracking.

General observations and edge cracking monitoring

- The southwest (SW) quadrant of site 4 was observed to have a relatively high flow (2.4 ml/s) out of its ABS edge drain pipe about two to three hours after a heavy rain event.
- Minor edge cracking was observed at sites 4 and 6 in May 2016. Severe edge cracking (up to 10 cm wide) was found approximately 40 m north of site 6. Some of the edge cracking noticed outside of sites 4 and 6 was deep enough to have reached the subbase layer (i.e., 15+ cm deep). Figure 8 illustrates edge cracking on sites 4 and 6. It was also noticed that edge cracks on treated sites 4 and 6 appear less severe than the cracks on untreated sections.



Figure 8. Edge cracking at site 6 looking south (left), and at site 4 looking north (right), spring 2016.

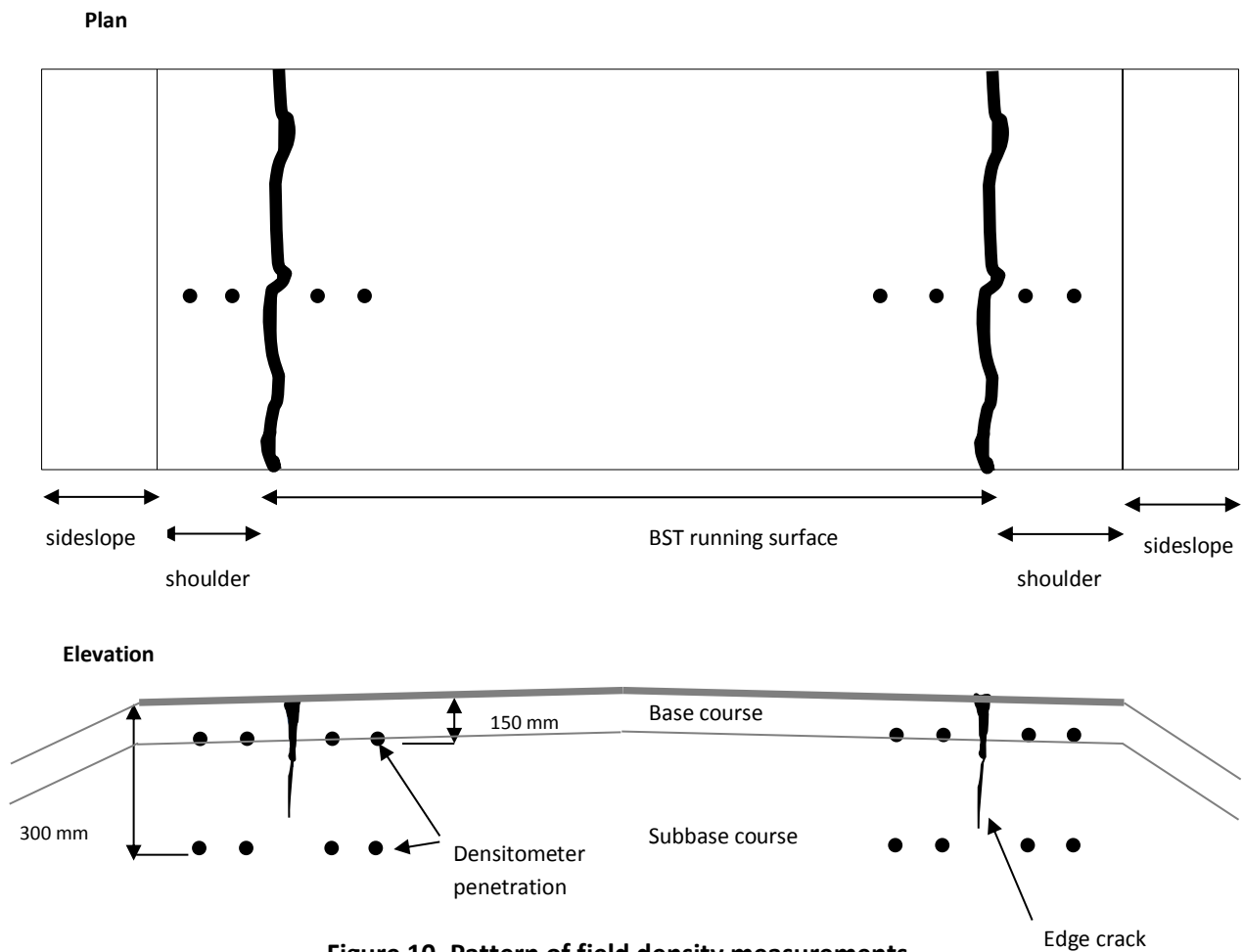
Field density study

A brief field study, with a nuclear density gauge, was conducted in September 2016 to document roadbed density differences between the road running surface and the road shoulder. Figure 9 illustrates the procedure for collecting field density measurements to either side of edge cracks using a nuclear density gauge. Field density tests were conducted on 2 different sites. The first field density test was conducted at a location immediately south of site 4 (at km 40), where both sides of the highways had edge cracking. The second field density test was conducted approximately 25 km north of site 6 (at km 66.275), where severe edge cracking was also present. The sideslope at km 40 was 3:1 whereas the pavement at km 66.275 was on a deep fill and had a sideslope of 2:1. At each site, field density measurements were conducted on both sides of the road, at two points on each side of the edge cracking. Figure 10 illustrates the field density test matrix used. Density measurements were gathered

for rod penetration depths of 150 and 300 mm from the top of the base course (after removing the BST, if necessary).



Figure 9. Measuring road density with a nuclear density gauge (left), and edge crack filled with gravel (right) at km 40.



Density measurement with the nuclear density gauge provided information on soil density, percentage of compaction as well as moisture content. Figure 11 summarises the results of the field density survey. The average dry density for each test was normalized relative to the dry density of a reference point, which was taken to be the measurement point closest to centreline, on each side of the road, at the same depth. (These reference test points are coloured red in Figure 11). Normalizing the field densities highlights the progression of decompaction from the running surface to the edge crack and to the road shoulder.

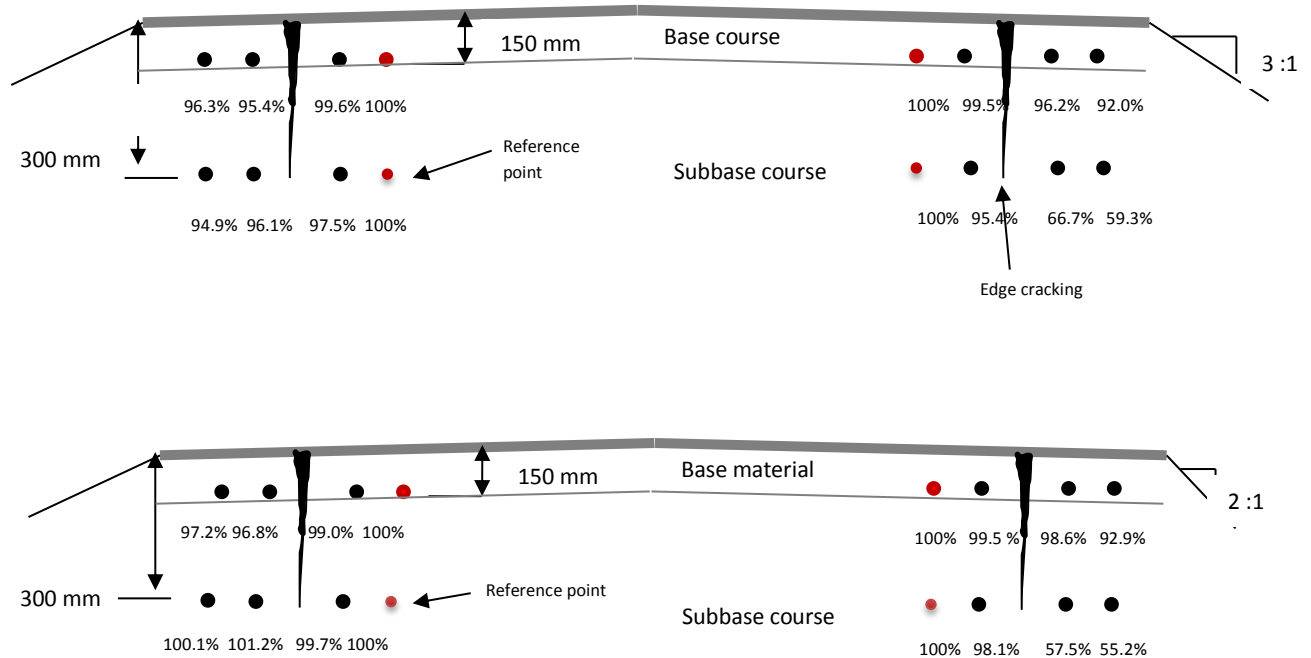


Figure 11. Relative dry density of roadbed materials at km 40 (top) and km 66.275 (bottom).

Two trends were observed in the data from the field density study:

- Materials outside of the edge crack were less dense than inside (i.e., closer to the road centre). Base materials were as much as 8% less dense outside of edge cracks, whereas the uppermost 150 mm of subbase material was as much as 45% less dense outside of edge cracks.
- The level of compaction in the road increased from the surface downwards. Comparing the reference points of site 4, the base course dry densities were 85% to 90% of the corresponding subbase dry densities. Km66+275 showed a negligible difference for the reference densities on the cutslope side of centerline; however, because of very high subbase densities the base course was only 55% of the subbase reference density on the steep slope side.

The most advanced state of edge cracking was noticed on the fill slope side of the road section located at km 66.275. Both site 4 and the site at km 66.275 had dramatically reduced soil densities (55%-59%) outside of edge cracks in the top of the subbase. The road at km 66.275 had a deeper fill and steeper sideslope than at km 40. At this time, it is difficult to correlate the level of compaction with sideslope. However, there is strong evidence that there is a relationship between a roadbed's level of compaction and its porosity and ability to soak up precipitation. Less dense roadbed materials have a more open

structure that will soak up more surface runoff and may, depending on the gradation and pore sizes, promote capillary rise of ground water.

General trends from temperature and moisture data analysis

The following observations about temperature and moisture data collected at sites 4 and 6 apply to the period of September 2015 to mid-January 2017. The data acquisition systems were programmed to record moisture content and temperature data hourly from the sensors.

- **General temperature trends**

The maximum and minimum temperature profiles presented in Figure 12 show a wide range of temperatures occurred at the test sites during the study period. The maximum variation occurred near the road surface, and this variation grew less with depth—forming a ‘trumpet’-shaped curve. The maximum air temperature range was 37°C to -29°C, and was recorded by the ambient thermistors at the dataloggers. Because the maximum temperatures at the 1.6 m depth exceed 0°C it is apparent that the road is not underlain by permafrost. Although the maximum and minimum ambient temperatures were comparable for the two sites, the site 4 roadbed temperature extremes were almost all cooler than those at site 6.

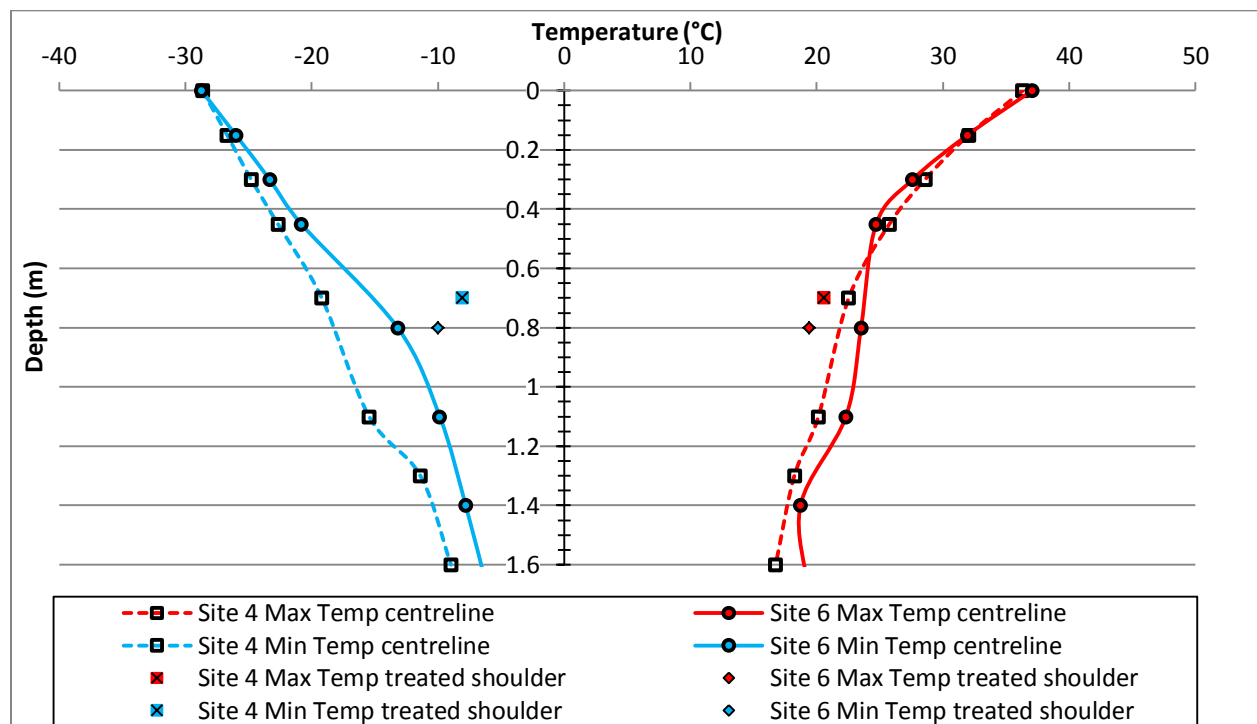


Figure 12. Centreline and shoulder temperature ranges with depth, sites 4 and 6, 2016.

Figure 13 presents temperature results at select depths for site 6 during fall 2015. As anticipated, there was greater temperature variation at shallow roadbed depths where solar heating and ambient cooling bring about rapid changes in the roadbed. The road shoulder had consistently cooler temperatures than at centreline during fall 2015. This is attributed to the road shoulder having lower soil densities and wetter soil conditions, but may also be caused by the road surface receiving more direct solar input.

Figure 14 presents results for the same site 6 thermistors, for winter and spring 2016. Similar to Figure 13, Figure 14 illustrates that shallow roadbed depths have higher sensitivity to air temperature variation, and also shows top-down freezing and thawing events. It is important to note that the road surfaces at sites 4 and 6 were unpaved for the periods shown.

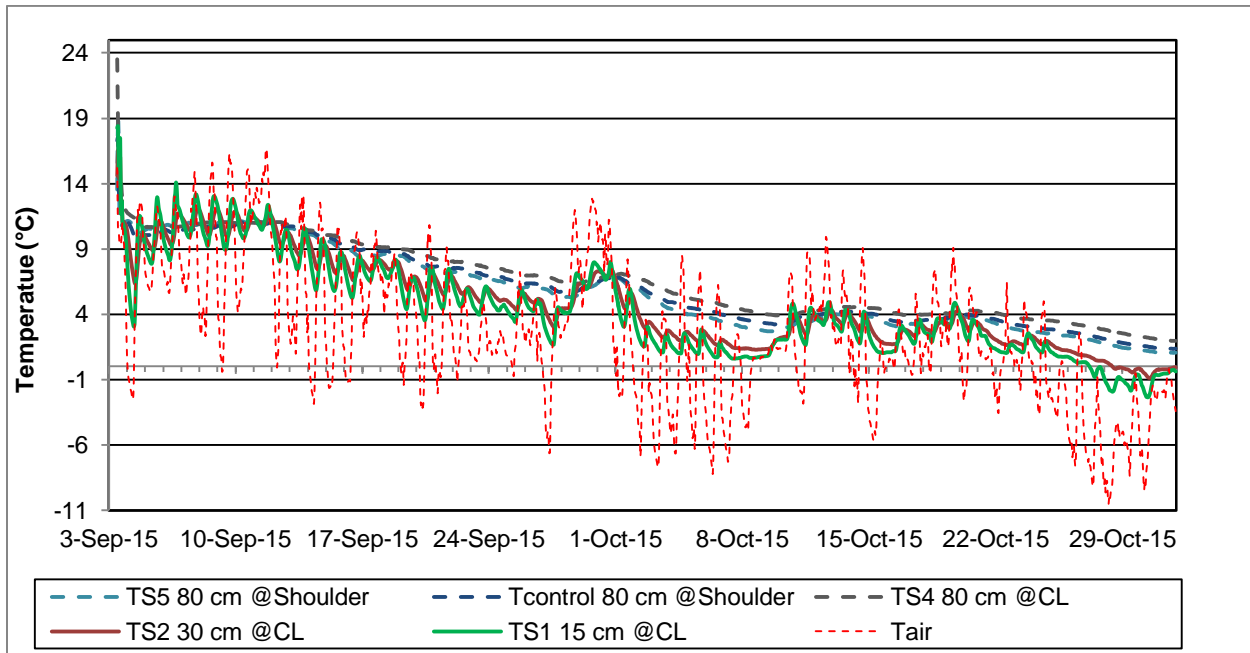


Figure 13. Temperature data, site 6, fall 2015.

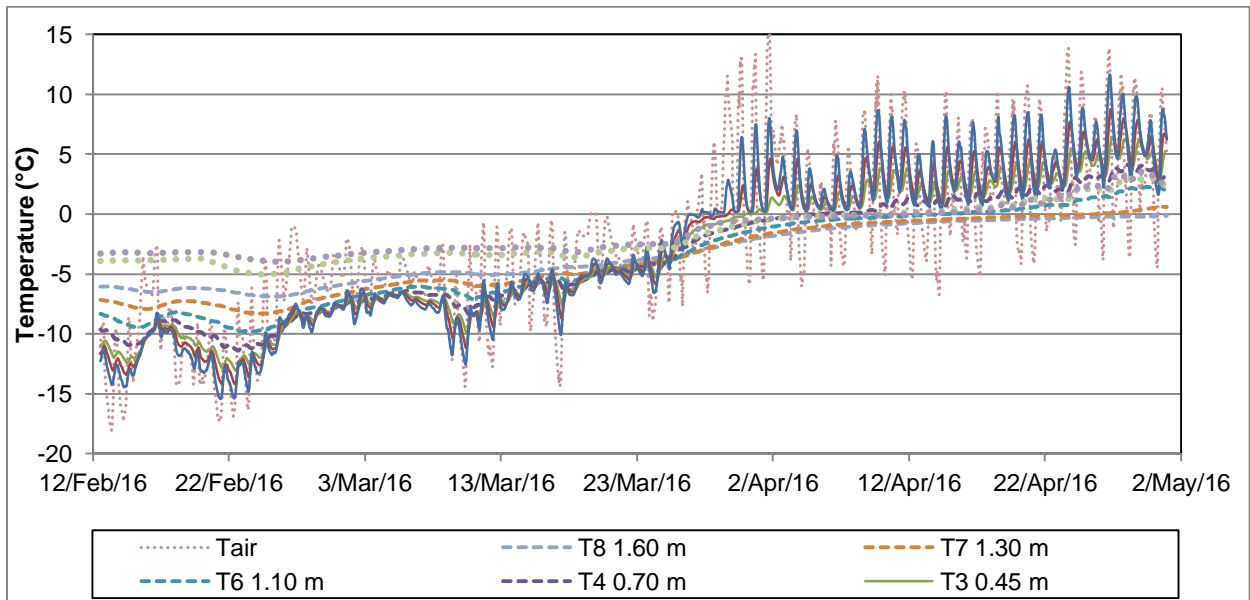


Figure 14. Temperature data, site 4, spring 2016.

Knowing that edge cracking develops along the Campbell Highway between March and May, a correlation was sought between roadbed temperature and time. Figure 15 compares centreline and shoulder temperatures at site 4 during late winter to spring 2016. Centreline temperature was as much as 5°–6° C colder than the shoulder in the winter. The main reason for the differences between

centreline and shoulder temperatures is believed to be the insulating effect of compact snow and ice accumulated on the road shoulders by winter maintenance. The presence of snow on the road shoulders both created a temperature differential between centreline and shoulder, and eliminated diurnal temperature fluctuation at the road shoulder. The shoulder temperatures fluctuated slowly during the winter and in Figure 15 appear as very smooth lines. In contrast, the centreline temperature appears as a very jagged line indicating rapid, diurnal, variation in the absence of snow on the road surface. On March 13, a snow plow removed most of the snow from the road shoulder and this initiated diurnal temperature variation in the shoulder at 0.7 m depth. This diurnal variation continued until a snow event from March 19 to March 21 again provided shoulder insulation. By March 26 the roadbed started to melt despite there being some snow cover on the road shoulder—temperatures at centreline and shoulder rose together. On April 7, spring maintenance was conducted to remove deep snow from the road shoulder and sideslope by blading and winging it to the back slope of the ditch (Figure 16). The lines for centreline and shoulder temperature at 0.7 m started to display diurnal temperature variation on April 8 and April 16, respectively, when they thawed.

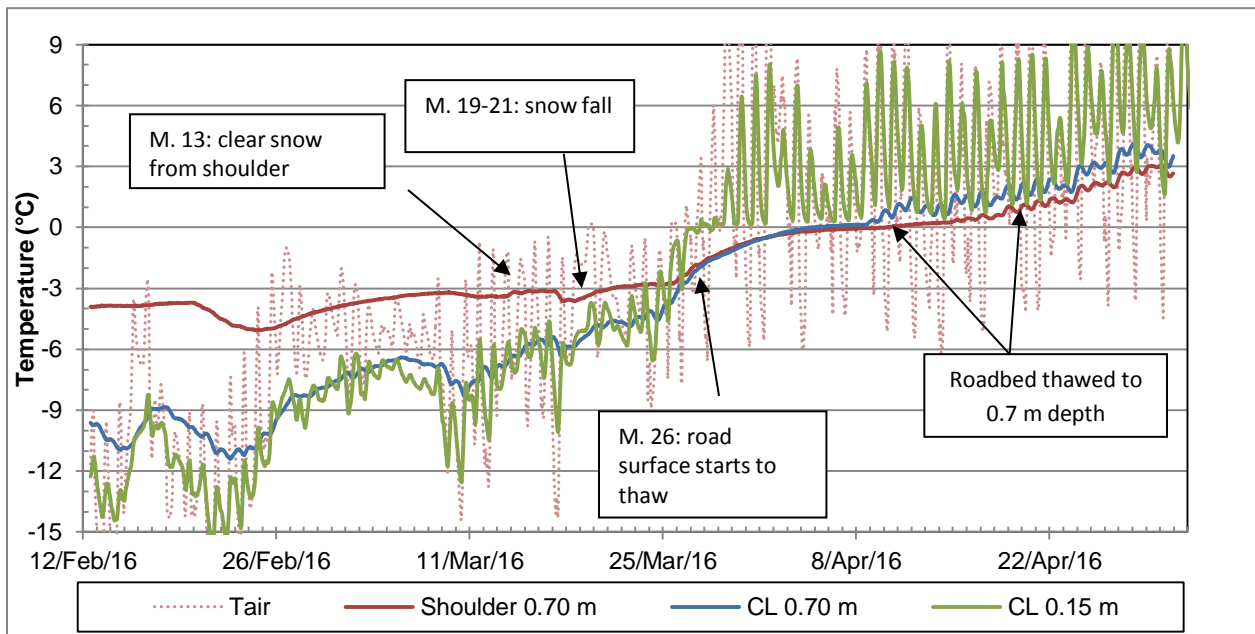


Figure 15. Temperature at shoulder and centreline, site 4, late winter- early spring 2016.



Figure 16. Blading and winging snow off of the road shoulder and sideslope, 7 April 2016.

- **General moisture trends**

Figure 17 below presents moisture data from site 4 during spring 2016 and compares road centreline to road shoulder at two different depths. The centreline thawed several days before the road shoulder, and the untreated shoulder thawed slightly slower than did the shoulder with Mirafi® H₂Ri. Under the Mirafi® H₂Ri geosynthetic at site 4 (at a depth of 0.7 m), the roadbed thawed nine to ten days earlier at centreline than at the road shoulder. Higher moisture levels were recorded at 0.7 m than at 0.3 m and 0.4 m. This is likely because, at deeper depths, there are more fine grained soils and these retain more moisture but may also be due to the action of the Mirafi® H₂Ri geosynthetic. The moisture contents of the frozen shoulder also were higher than at centreline indicating a wetter fall condition and, possibly, that more water migrated to the freezing front in the shoulder due to its more porous condition. An analysis of temperature data, presented in Figure 15 for the same spring 2016 period, showed that the centreline thawed faster than the shoulders. This statement is substantiated by the thawing patterns illustrated in Figure 17. On both charts, thawing starts on March 25, 2016.

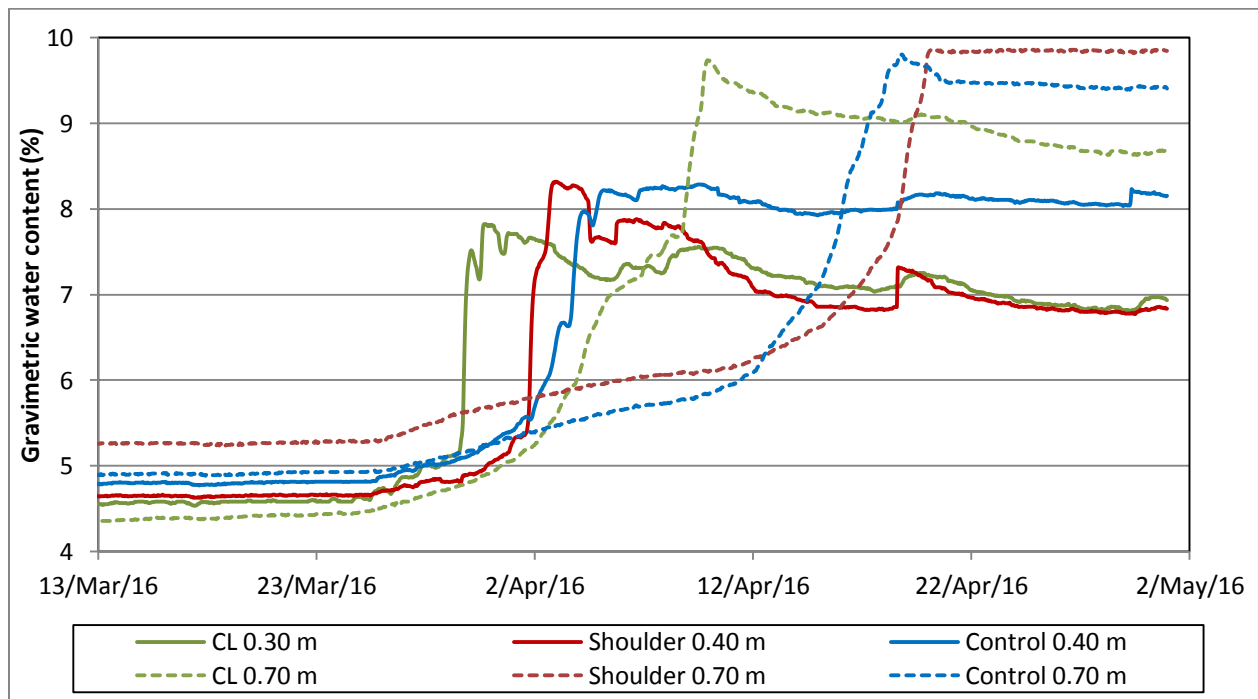


Figure 17. Moisture data, site 4, spring 2016.

Another important finding illustrated by Figure 17 is the ability of the geosynthetic to drain the roadbed. At both centreline (0.3 m) and shoulder (0.4 m) of the treated site, after the release of water by thawing, the moisture contents decreased by 1% to 1.5% indicating the geosynthetic was helping to drain the roadbed. In contrast to this, after thawing of the untreated shoulder, the excess water did not drain away. Also, field density tests show strong evidence of the shoulders being less compacted and, therefore, hold a higher void index, which has a tremendous impact on freezing. Therefore, based on increasing shoulder temperatures and moisture contents, the treated and untreated sections started thawing at the same time at both site 4 and site 6. This is believed to have occurred when the snow had melted away from on the shoulder. Also, thawing started at the shoulder of site 4 when temperatures at 0.4 m were about at -2°C (March 25th). A likely explanation of this is that soil salinity was considerable, and this lowered the freezing and thawing set points to below 0°C.

- **Impact of Bituminous Surface Treatment (BST) application during summer 2016**

After construction of the test sites were completed in fall 2015, BST was applied to sites 4 and 6 on June 16, 2016. It was anticipated that a difference in solar gain on the road surface would be noticed after BST application. Figure 18 illustrates the impact of BST application on moisture and temperature at site 4. Site 6 had comparable results. After the BST application, centreline materials between the paved surface and the geosynthetic stopped experiencing wetting from rain events and slowly dried. This occurred because, after BST application, the soil at 30 cm on centreline was sealed between two impervious layers. This illustrates the impact of the BST which was to retain more solar energy and increase roadbed temperature. Roadbed heating due to the BST was also observed at 0.45 and 0.70 m depths in the road, but to a lesser extent.

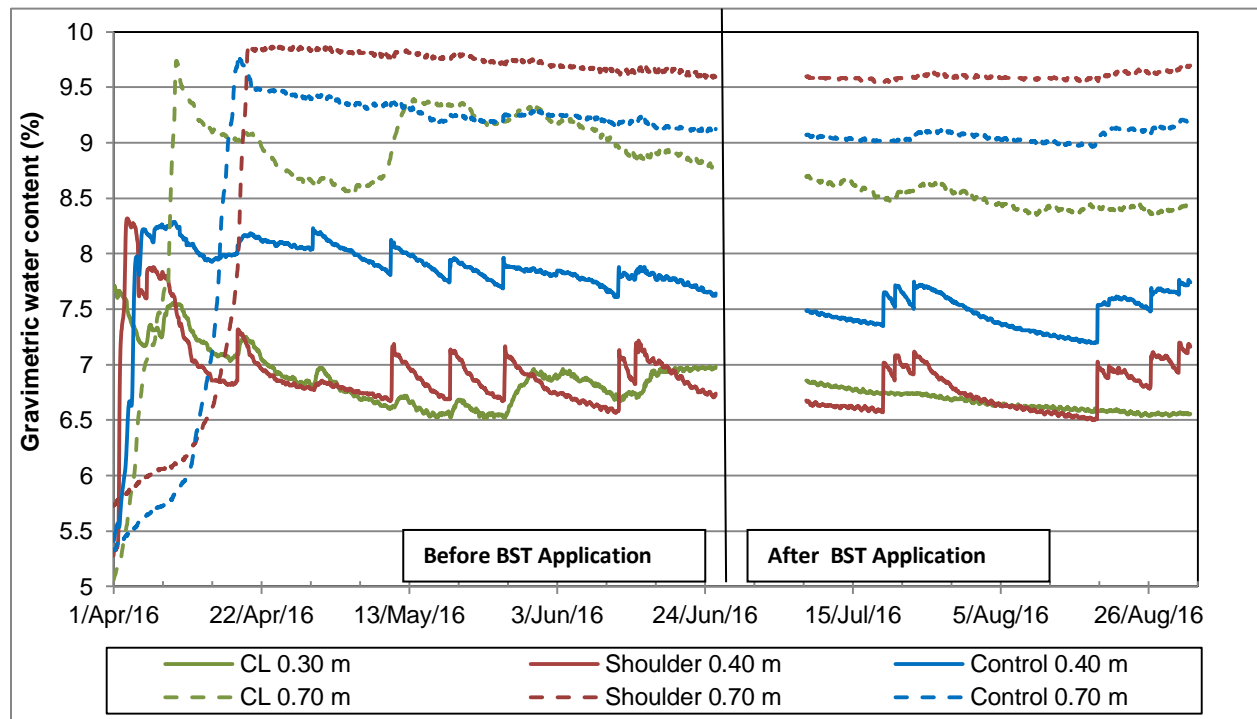


Figure 18. Moisture data, site 4, summer 2016.

DISCUSSION

Analysis of the impact of the Mirafi® H₂Ri geosynthetic on road performance

The Mirafi® H₂Ri draining and wicking properties, as well as the product’s ability to prevent or reduce edge cracking, are being studied.

- **Validation of Mirafi® H₂Ri wicking and draining properties**

Figure 18 presents moisture levels for site 4 during spring and summer 2016. The chart illustrates moisture levels above and under the geosynthetic both at the road centreline and the road shoulder (on the treated and untreated sections). Starting on March 25, frozen water in the roadbed started melting and being released at the thawing front as top-down thawing began. Moisture contents reached 7.8%

and 8.2%, respectively, at the road centreline (0.3 m) and the treated shoulder (0.4 m). Approximately 10 days later, a percentage of the moisture had dissipated and moisture contents were down to 6.8%, both at road centreline and treated shoulder. On the untreated shoulder, however, moisture content at 0.4 m depth increased to 8.2% after thawing but remained at this high level of moisture throughout the spring period. This is a strong indication of the ability of the Mirafi® H₂Ri geosynthetic to drain excess water that accumulates at the thawing front during spring top-down thawing. The geosynthetic also appears to drain water (and potentially to interrupt capillary rise) from the underlying roadbed materials. With reference to Figure 17, spring thaw moisture levels just under the geosynthetic at centreline at Site 4 peaked to 9.6% and then dropped to 8.6% in two weeks. Site 6 peaked to 9.6% and then dropped to 9.1% in three weeks. At both sites, moisture levels in the road shoulder, with or without geosynthetic, showed little to no drainage for the same time period. This is presumably because of prolonged frozen soil conditions followed by a relatively high water table in the ditch. During summer, the patterns of drainage initiated in the spring continued. At site 4, the lowest summertime moisture content was 6.5% and this occurred at both the centreline (0.3 m depth) and the shoulder (0.4 m depth). A number of factors caused this drying—the most important being the geosynthetic and roadbed heating due to high summer air temperatures and increased heat adsorption after the BST application. In this well-drained condition, the roadbed materials are near to their optimum moisture content and would have increased matric suction—both of which improve the strength and stability of the roadbed.

During spring and summer, the test site roadbeds above the geosynthetic experienced recurrent, rapid increases and decreases in moisture content (Figure 18). Moisture changes were, on average, 0.12% greater in the drier roadbed of the treated shoulder than in the wetter, untreated shoulder (May to September). The treated shoulder also drained away these increases in moisture more quickly than did the untreated shoulder. In order to better understand these events, a comparison with precipitation data was made. Precipitation data for the summer period were from Environment Canada's weather station located at Watson Lake airport (the Environment Canada weather station closest to sites 4 and 6). Figure 19 compares summer moisture contents at sites 4 and 6 with summer precipitation events. There was strong agreement between the precipitation events and increases in moisture above the geosynthetic. As anticipated, the agreement was weaker for moisture content under the geosynthetic.

- **Ability of the geotextile to prevent or reduce edge cracking**

The main finding was that a difference in moisture level between the road running surface and the road shoulder is potentially not the main reason for edge cracking. Various results detailed in this paper demonstrated that the geosynthetic wicking and draining properties are working well. Roadbed moisture was well controlled through these actions of the geosynthetic. Although it reduced roadbed moisture levels, the action of the geosynthetic in the test sections might not be sufficient to prevent edge cracking. During spring 2016, some minor edge cracking was observed on the treated shoulders of sites 4 and 6. Although more severe edge cracking was found in nearby untreated road sections, it is premature to make a statement on the ability of the Mirafi® H₂Ri to eliminate or reduce edge cracking. HPW noted that edge cracking may take as long as five years to manifest after road construction.

According to TenCate, manufacturer of the Mirafi® H₂Ri, studies are still being done on the optimum placement of the geosynthetic. This brings into question the placement of the geosynthetic at 69 and 79 cm of depth, respectively, at sites 4 and 6. If the geosynthetic had been placed closer to the road surface, this may have prevented cracking by laterally confining the shoulder materials and draining the top of the shoulder. The optimal depth to achieve both shoulder reinforcement and roadbed drainage has not yet been determined for these sites.

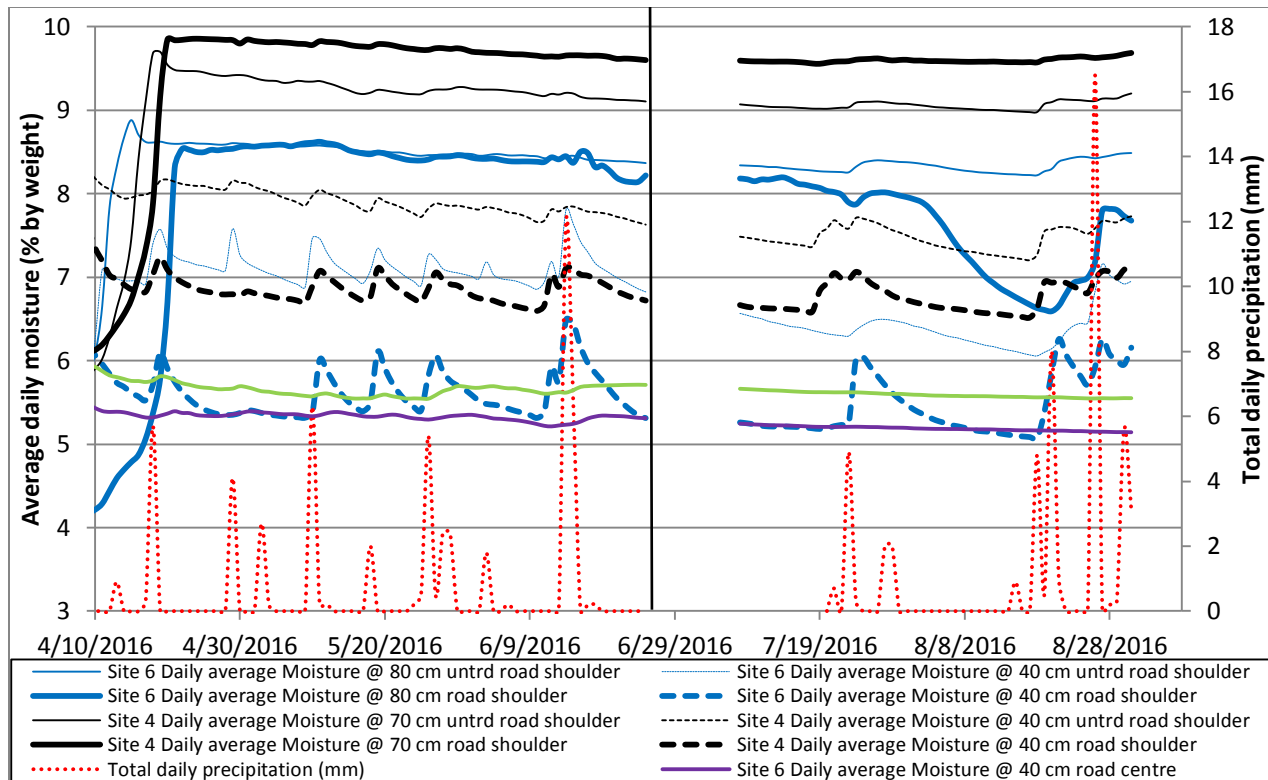


Figure 19. Comparison of precipitation and road moisture, sites 4 and 6, spring and summer 2016.

- **Potential Other Causes of Edge Cracking on Northern Roads**

Apart from the action of high moisture contents in the road shoulder during spring, aspects of roadbed material properties, maintenance practices, road geometry, and traffic action also may contribute to edge cracking (Bradley et al. 2015). These mechanisms are independent of the performance of the geosynthetic and include:

Differential compaction. Large differences in compaction between road shoulders and sideslopes, and the adjacent running lane materials. Noted by HPW, and observed in field density measurements performed in this phase, road shoulders and side slopes may have much lower densities than materials towards the centre of the road. One cause of this differential compaction is that heavy vibrating drum compactors cannot safely compact along the outside edges of lifts where the materials are not laterally confined. Efforts to do this may result in heavily overcompacted materials just inside the edge and undercompacted materials immediately outside of this. As noted by Thiam (2014) under-compacted roadbed materials have higher hydraulic conductivity and this causes them to intercept and retain more road surface runoff. Given large differences in compaction, the completed roadbed would tend to shrink and swell differentially at the road shoulders, and cracks between the dense and less dense materials develop.

Road prism side slope. Preliminary observations from site monitoring suggest that steeper slopes increase edge cracking susceptibility. According to HPW, highway construction specifications require secondary highway sideslopes over 2 m high to be constructed at 2:1 and sideslopes fewer than 2 m high to be constructed at 3:1. In contrast, primary highway sideslopes are constructed at 4:1. Severe cracking has occurred at km 66.275 of the Campbell Highway where there is a high 2:1 sideslope. Much less severe cracking was observed on the uphill, 3:1, sideslope at the same site. Sites 4 and 6 also were

built with a 3:1 side slope. No edge cracking has been observed by YG HPW on nearby, BST or HMA sections of the Alaska highway built with 4:1 side slopes. These road sections have comparable weather and roadbed materials. Steeper side slopes may promote edge cracking by reducing the stability of sideslope and shoulder materials such that they rotate outwards and (or) creep downslope. The Alaska Highway has a wider roadbed and much more traffic.

CONCLUSIONS

This paper summarises results from the second phase of a study of edge cracking on northern highways, and their control with Mirafi[®] H₂Ri, a new wicking geosynthetic product from TenCate. Detailed analyses were conducted of moisture and temperature data from two instrumented test sites, in conjunction with monitoring of surface distress at these sites. The objective was to use information gathered from the data analyses, and extended with site observations, to evaluate the geosynthetic's ability to drain the road and to prevent edge cracking. From the combination of site monitoring and data analysis, it has been concluded that the geosynthetic is draining moisture effectively. It is more difficult to state whether the geosynthetic, as installed, is effective at preventing or reducing edge cracking. Minor edge cracking appeared in spring 2016 at both of the treated test sites, but it is not yet clear whether the geosynthetic reduced the severity of cracking. However, preliminary observations indicate that the treated sections experienced less cracking than the untreated sections. Monitoring during spring 2017 will help make a more definitive statement about the ability of the Mirafi[®] H₂Ri geosynthetic to prevent edge cracking. Field density surveys of road edge materials found lower levels of compaction outside of edge cracks and at the road shoulder, and at shallower depths of the highway. Road sections with steeper sideslopes appeared to be more susceptible to severe edge cracking, and this may be related to construction practices.

This project is still ongoing and the next step consists of having a closer look at moisture and temperature data, combined with site monitoring in order to validate and confirm theories about edge cracking formation and strategies for their mitigation. A series of activities will take place in the future and a focus will be made on the effect of geometry, construction, snow maintenance, installation of geosynthetic, soil density, roadbed water flow, and spring thaw effects.

REFERENCES

- Bradley, A.H.; Thiam, P.M.; Drummond, S. 2016. "Mitigating pavement cracking during thaw by controlling roadbed moisture with wicking geosynthetics on low volume roads in the Yukon: Phase 1—construction". Contract Report 11288, FPInnovations, Pointe Claire, QC.
- De Guzman, E.M.; Piamsalee, A.; Alfaro, M.; Arenson, L.; Dore, G.; Hayley, D. 2015. "Initial monitoring of instrumented test sections along the Inuvik-Tuktoyaktuk highway". Paper for GEOQuebec 2015. 7 pp.
- Thiam, P.M. 2014. "Effect of the future increase of precipitations on the long-term performance of roads". Master Thesis. Laval University. Quebec. 124 pp.
- Yukon Government. "Yukon Traffic Count Summary 2011". Transportation Planning and Programming, Transportation Engineering Branch. Yukon Highways and Public Works. Whitehorse, Yk. 170 pp. Accessed at <http://www.hpw.gov.yk.ca/pdf/traf2011.pdf>